



# Imaging evaluation following transarterial radioembolization with yttrium-90 microspheres downstaging hepatocellular carcinoma: the first case in China

Xiaoming Li<sup>1#</sup>, Xuantong Yue<sup>2#</sup>, Lin Zhang<sup>3</sup>, Chen Liu<sup>1</sup>, Jian Wang<sup>1</sup>, Hui Zhang<sup>4</sup>, Ping Cai<sup>1</sup>

<sup>1</sup>Department of Radiology, Southwest Hospital, Third Military Medical University (Army Medical University), Chongqing, China; <sup>2</sup>Department of Radiology, Sichuan Science City Hospital, Mianyang, China; <sup>3</sup>Hepato-pancreato-biliary Center, Beijing Tsinghua Changgung Hospital, School of Medicine, Tsinghua University, Beijing, China; <sup>4</sup>The Institute of Hepatobiliary Surgery, Southwest Hospital, Third Military Medical University (Army Medical University), Chongqing, China

<sup>#</sup>These authors contributed equally to this work.

*Correspondence to:* Hui Zhang. The Institute of Hepatobiliary Surgery, Southwest Hospital, Third Military Medical University (Army Medical University), Chongqing, China. Email: 13637912611@163.com; Ping Cai. Department of Radiology, Southwest Hospital, Third Military Medical University (Army Medical University), Chongqing 400038, China. Email: 530305942@qq.com.

Submitted Sep 09, 2022. Accepted for publication Jan 11, 2023. Published online Feb 09, 2023.

doi: 10.21037/qims-22-943

**View this article at:** <https://dx.doi.org/10.21037/qims-22-943>

## Introduction

Hepatocellular carcinoma (HCC) is one of the most malignant tumors, the morbidity and mortality of HCC ranked 6th and 3rd among all malignant tumors, respectively. Patients with HCC in Asia tend to have poorer liver function and present at a more advanced stage than patients in Western countries (1). Approximately 70–90% of patients with HCC in Asia are co-infected with the hepatitis B virus (HBV). The percentage of Chinese HCC patients who have HBV infection is estimated to account for approximately 75–80% in China (2). Furthermore, Asian and Western countries have different staging systems, disease management practices, and prognoses for HCC. Transarterial radioembolization with yttrium-90 microspheres (TARE-Y90) has been used to treat HCC in Western countries for 20 years, and Chinese guidelines for HCC management also recommend yttrium-90 as a local treatment (3). However, there are no studies on the use of TARE-Y90 in China.

As a local treatment, TARE-Y90 can be applied to all BCLC (Barcelona Clinic Liver Cancer) stages of HCC (4). It has become an effective alternative to conventional transcatheter arterial chemoembolization, with better

time-to-progression and survival (5). In addition, TARE-Y90 can be used as a second option for patients with contraindications to radiofrequency ablation or surgical resection (6,7). Furthermore, it is also a suitable strategy for treating HCC with portal invasion, with minimal incidence of ischemic hepatitis (4).

This case report describes the case of the first patient with HCC to receive TARE-Y90 treatment in China. Throughout the treatment process, imaging was employed as an essential technical tool, providing an important basis for the assessment of the tumor response. Herein, we describe the oncological benefit, choice of imaging technique, tumor response assessment, and benign imaging findings of the patient after TARE-Y90 treatment.

## Case report

All procedures performed in this study were conducted in accordance with the ethical standards of the institutional and/or national research committee(s) and with the Helsinki Declaration (as revised in 2013). Written informed consent was obtained from the patient for the publication of this case report and the accompanying images. A copy of the written consent form is available for review by the editorial

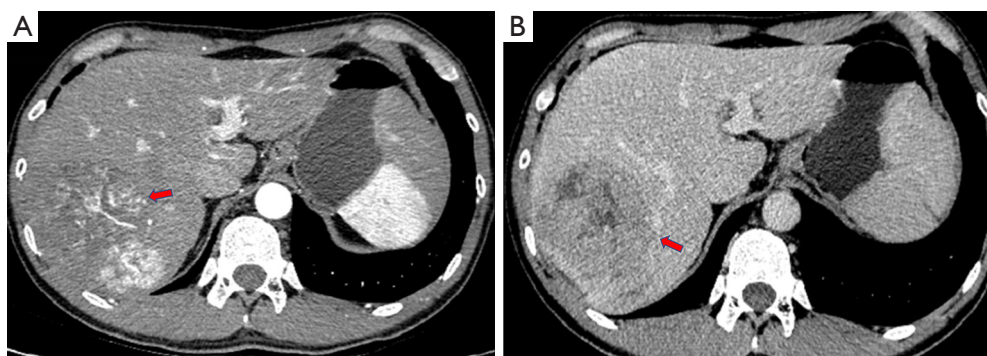


**Figure 1** Contrast-enhanced CT scans of the HCC. (A) The mass shows non-rim arterial phase hyperenhancement in the arterial phase (red arrow). (B) The mass shows nonperipheral wash-out in the portal venous phase, with invasion of the portal vein (red arrow). CT, computed tomography; HCC, hepatocellular carcinoma.

office of this journal.

### *Patient information*

A 35-year-old male patient presented with a liver mass, recurrent distending pain in the liver area, and no history of chronic liver disease or long-term heavy alcohol drinking. Routine laboratory test results at admission showed the following abnormal results: positivity for HBV components including HBsAb (+), HBeAb (+), and HBcAb (+); alanine aminotransferase 73.8 IU/L (normal range, 0–42 IU/L); aspartate aminotransferase 49.3 IU/L (normal range, 0–42 IU/L); glutamyl transpeptidase 102.8 IU/L (normal range, 4–50 IU/L); alpha-fetoprotein (AFP) 175,499 ng/mL (normal range, 0–8 ng/mL); and protein induced by vitamin K absence-II (PIVKA-II) 11,082 mAU/mL (normal range, 0–40 mAU/mL). The other laboratory test results, including liver and kidney function, coagulation tests, HBV-DNA replication, and routine blood tests, were normal.

Imaging examination, including contrast-enhanced computed tomography (CT), indicated a heterogeneous, low-density mass with areas of necrosis measuring 10.2 cm in the right liver. The mass showed non-rim arterial phase hyperenhancement with multiple tortuous vessels in the arterial phase and nonperipheral wash-out in the portal venous phase, and malignant portal vein thrombosis (Figure 1). The patient had no cirrhosis, splenomegaly, ascites, or esophageal or gastric varices.

### *Preoperative evaluation and surgical procedure*

The patient was diagnosed with HCC (BCLC-C), with

Child-Pugh A liver function, a performance status score of 0, and an indocyanine green retention test value of 4.9%. By measuring the right hepatectomy, the future liver remnant was only 25%. Owing to the insufficient future liver remnant, the HCC was determined to be unresectable. After referring to the foreign clinical practice standards (7), we found the patient to be fully eligible for TARE-Y90 treatment. Routine angiography was performed 2 days before the TARE-Y90 therapy to exclude anatomical variation in the hepatic artery. A single-photon emission CT examination with  $^{99m}\text{Tc}$ -MAA was performed, and the lung-shunting fraction was found to be 15.1% [lung-shunting fraction = counts in the lungs/(counts in the lungs + counts in the liver)  $\times$  100%], without intra/extrahepatic shunts. A microcatheter was accurately inserted into the feeding artery of the tumor, and 2.01 GBq  $^{90}\text{Y}$  resin microspheres were injected into the tumor. The total operation time was less than 1 hour and no intraoperative adverse effects occurred. Single-photon emission CT was performed 20 hours after the operation, and no extrahepatic distribution of  $^{90}\text{Y}$  microspheres was observed. After 2 days, the AFP level decreased to 141,000 ng/mL.

### *Postoperative follow-up*

After the TARE-Y90 therapy, the patient was followed up by telephone once a week. Tumor markers, laboratory tests, and imaging examinations, including CT and hepatobiliary contrast agent magnetic resonance imaging (HBA-MRI), were performed monthly (Table 1). The details of the patient's imaging manifestations are shown in Figure 2. At 3 months after treatment, the tumor size was reduced by 31%, there was no enhancement, and the portal vein thrombosis

**Table 1** Imaging manifestations at 1<sup>st</sup> month, 2<sup>nd</sup> month and 3<sup>rd</sup> after TARE-Y90 treatment

Variable	1 <sup>st</sup> month	2 <sup>nd</sup> month	3 <sup>rd</sup> month
AFP (ng/mL)	10,612	1,469	325
PIVKA-II (mAU/mL)	329	27	None
Child-pugh	A	A	A
CT manifestations			
Density	Low density, with slight high density	Low density, with slight high density	Low density, with slight high density
Length (cm)	6.2	6.2	4.3
Residual enhancing areas (cm)	4.2	2.1	None
Enhancement pattern	Wash-in and wash-out	Wash-in and wash-out	None
Peritumoral ring enhancement	None	Present	Present
Portal vein invasion	None	None	None
Peri-tumor liver parenchyma	Type I	Type I	Type I
Other sign of liver parenchyma	None	"Ill-defined geographic areas" of hypoattenuation of segment VI on contrast scan	The abnormal enhancement range has been reduced
Extrahepatic signs	None	None	None
HBA-MRI manifestations			
T <sub>1</sub> WI	Hypointensity, with hyperintensity	Hypointensity, with hyperintensity	Hypointensity, with hyperintensity
T <sub>2</sub> WI	Hyperintensity	Hyperintensity	Hyperintensity
Residual enhancing areas (cm)	4.4	2.3	None
Enhancement pattern	Wash-in and wash-out	Wash-in and wash-out	None
Peritumoral ring enhancement	None	Present	Present
Peritumoral hypointensity on hepatobiliary phase	Present	Present	Present
SWI	Hypointensity	Hypointensity	Hypointensity
DWI (b=800 s/mm)	Hyperintensity	Hyperintensity	Hyperintensity
Other sign of liver parenchyma	None	"Ill-defined geographic areas" of hypoattenuation of segment VI	The abnormal enhancement range reduced
Extrahepatic signs	None	None	None

TARE-Y90, transarterial radioembolization with yttrium-90 microspheres; AFP, alpha-fetoprotein; PIVKA-II, protein induced by vitamin K absence-II; CT, computed tomography; HBA-MRI, hepatobiliary contrast agent magnetic resonance imaging; T<sub>1</sub>WI, T1-weighted imaging; T<sub>2</sub>WI, T2-weighted imaging; SWI, susceptibility weighted imaging; DWI, diffusion-weighted imaging.

had disappeared. These results were interpreted as a complete clinical response, and the HCC was downgraded to BCLC-A. The AFP level increased steadily to 491 and 605 ng/mL in the fourth and fifth months after the procedure, respectively; subsequently, a resection of the right posterior lobe was performed. Pathological results showed that most of the

tumor bed (96%) was necrotic. Microscopic residual tumor cells were observed at the tumor margin, with the largest foci measuring 2 mm, and yttrium-90 microspheres were observed in the capillaries of the peritumor tissue (*Figure 3*). At 3 months after resection, there had been no recurrence, as observed by HBA-MRI. At 8 months after resection, the

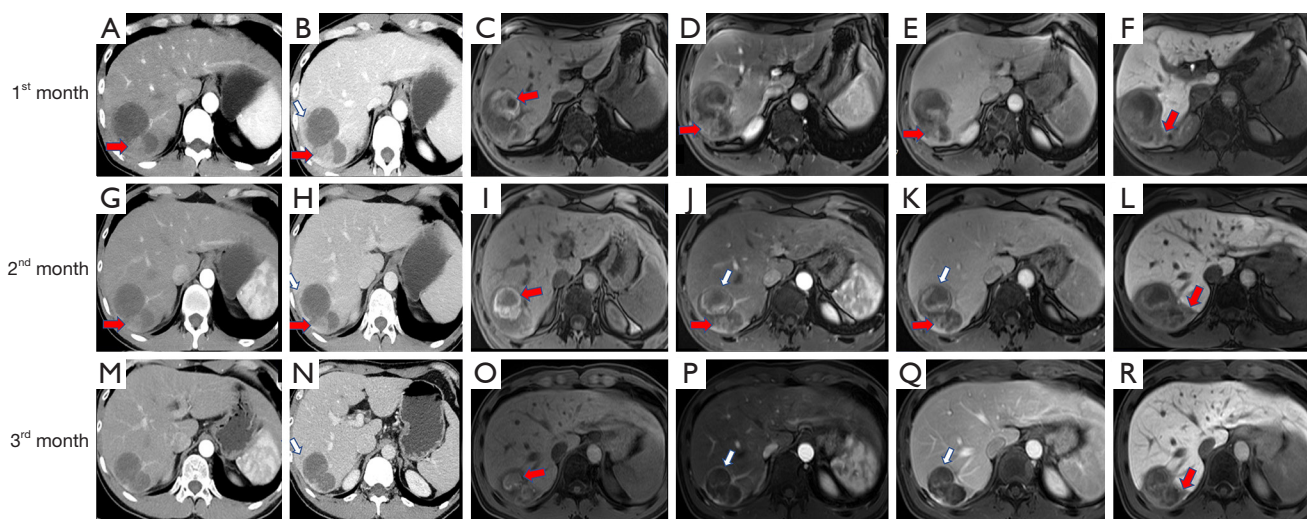


**Figure 2** CT and HBA-MRI manifestations the first month, second month, and third after TARE-Y90 treatment. In the first month after TARE-Y90 treatment, axial images show a residual tumor, hemorrhage, a type I enhancement pattern, and peritumoral hypointensity on HBP (A-F). Contrast-enhanced CT shows residual enhanced areas (4.2 cm) in the arterial phase (red arrow) (A). The enhancement pattern is “wash-in and wash-out” (red arrow). The peritumor liver parenchyma shows hypoattenuation in the portal venous phase (white arrow) (B). Precontrast MRI shows an intratumor hemorrhage (red arrow) (C) and a residual enhanced area in the arterial phase (red arrow) (D). The lesion shows “wash-out” in the portal venous phase (red arrow) (E). On HBP, peritumoral hypointensity relative to the liver parenchyma can be observed (red arrow) (F). In the second month after TARE-Y90 treatment, axial images show a residual tumor, hemorrhage, a type I enhancement pattern, peritumoral ring enhancement, and peritumoral hypointensity in the hepatobiliary phase (G-L). Contrast-enhanced CT shows the residual enhanced area (2.1 cm) in the arterial phase (red arrow) (G). The enhancement pattern is “wash-in and wash-out” (red arrow). The peritumor liver parenchyma shows hypoattenuation in the portal venous phase (white arrow) (H). Precontrast MRI shows an intratumor hemorrhage (red arrow) (I), a residual enhanced area in the arterial phase, and “wash-out” in the portal venous phase (red arrow), with peritumoral ring enhancement (white arrow) (J,K). On HBP, peritumoral hypointensity relative to the liver parenchyma can be observed (red arrow) (L). In the third month after TARE-Y90 treatment, axial images show a hemorrhage, type I enhancement pattern, peritumoral ring enhancement, and peritumoral hypointensity on the hepatobiliary phase (M-R). Contrast-enhanced CT shows hypodensity without residual enhanced areas in the arterial phase (M) and the portal venous phase. The peritumor liver parenchyma shows hypoattenuation (white arrow) (N). Precontrast MRI shows hyperintensity on T<sub>1</sub>WI, which represents an intratumoral hemorrhage (red arrow) (O), a lack of residual enhanced areas in the arterial and portal venous phases, and peritumoral ring enhancement (white arrow) (P,Q). On HBP, peritumoral hypointensity relative to the liver parenchyma can be observed (red arrow) (R). CT, computed tomography; HBA-MRI, hepatobiliary contrast agent magnetic resonance imaging; TARE-Y90, transarterial radioembolization with yttrium-90 resin microspheres; HBP, hepatobiliary phase; MRI, magnetic resonance imaging; T<sub>1</sub>WI, T<sub>1</sub>-weighted imaging.

patient had AFP and PIVKA-II levels within the normal ranges, and his general condition was good.

## Discussion

TARE-Y90 is an effective neoadjuvant therapy that can be undertaken before surgical resection and curative liver transplantation, making it a bridging and downstaging liver-directed therapy (8,9). Although TARE-Y90 has traditionally been used to treat advanced HCC, recent refinements of the technique have achieved promising

response rates in solitary HCC (10). Previous studies have shown that using TARE-Y90 can attain an objective response rate of above 85% (11,12) and a downstaging rate of above 50% (13,14). These high rates enable TARE-Y90 to be used as a bridging therapy prior to resection. After adjuvant treatment with TARE-Y90, our patient was assessed as having had a complete clinical response based on the activity of his HCC and portal vein thrombosis. The HCC was successfully converted from unresectable to resectable, representing the success of the downstaging treatment. As a result, the patient did not need concurrent

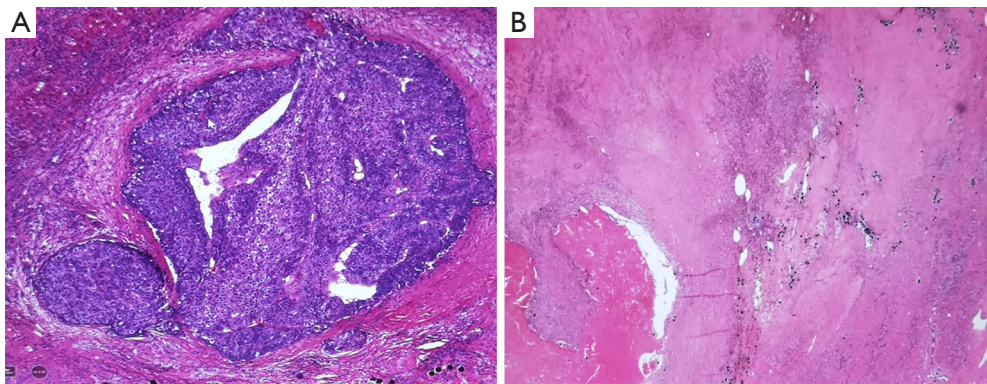


**Figure 3** Pathological examination after surgical resection of the right posterior lobe. (A) Pathological results show that most of the tumor bed was necrotic. Microscopic residual tumor cells were observed with a low-grade differentiation (HE,  $\times 200$ ), and (B) scattered yttrium-90 microspheres were observed in the capillaries of the peritumor tissue (HE,  $\times 100$ ). HE, hematoxylin-eosin.

systemic therapy, which is inconsistent with a previous report of that after TARE-Y90 treatment in conjunction with a neoadjuvant resulting in complete response (15). The success of this case suggests that more patients with similar conditions can be treated in the future, and new adjuvant applications of TARE-Y90 merit further study in China.

Several imaging techniques can be used to evaluate the postoperative performance of TARE-Y90, including ultrasound, CT, MRI, and PET-CT. Ultrasound imaging is economical and easy to perform but is limited to the value of the therapeutic response (16). Although PET-CT may be useful for stratifying patients before treatment and predicting outcomes (17), it has a low sensitivity (52%) for the detection of HCC, especially well-differentiated tumors (18). Dynamic contrast-enhanced CT is a convenient and efficient modality for assessing tumors after treatment (19). Compared to CT, MRI has increased sensitivity and similar specificity for detecting HCC, especially HBA-MRI, which can accurately identify small lesions ( $<1$  cm). A consensus has essentially been reached on current practices to evaluate the treatment response of TARE-Y90 with CT and MRI (20).

Regarding the response to TARE-Y90 treatment, the RECIST (Response Evaluation Criteria in Solid Tumors) guideline is inaccurate for assessing the response because intratumor hemorrhage and necrosis may cause an increase in tumor size after treatment (21). However, the modified RECIST criteria can accurately reflect the objective response rate by measuring the maximum enhanced diameter in the arterial phase (22). In our patient, no residual tumor activity was found on CT or MRI in the third month after treatment, which was interpreted as a

complete clinical response.

Other benign imaging findings after TARE-Y90 treatment include the following: (I) peritumoral ring enhancement ( $<5$  mm) lasting for up to 3 months, pathologically corresponding to granulation tissue and/or fibrous pseudo-envelope (23); (II) the irradiated hepatic parenchyma presenting with a type I enhancement pattern on CT, which may be caused by radiation-induced veno-occlusion, resulting in delayed contrast inflow (24); (III) peritumoral hypointensity in the hepatobiliary phase, indicative of hepatocyte dysfunction, which is caused by the ablative potential of Y90 microspheres (25); and (IV) the normal liver parenchyma appearing as “ill-defined geographic areas,” which may be caused by the embolic effect of Y90 microspheres and can cause infarcts, although the infarction will gradually recover through arterial recanalization and collateralization (26).

## Conclusions

TARE-Y90 is a potentially useful approach for treating unresectable HCC. The assessment of imaging manifestations, including tumor response and benign imaging findings, mainly through CT and MRI scans, can effectively determine the next treatment step.

## Acknowledgments

*Funding:* This study was supported by the Program of the National Natural Science Foundation of Chongqing (No. CSTB2022NSCQMSX1371).

## Footnote

*Conflicts of Interest:* All authors have completed the ICMJE uniform disclosure form (available at <https://qims.amegrouops.com/article/view/10.21037/qims-22-943/coif>). All authors report that this study was supported by the Program of National Natural Science Foundation of Chongqing (No. CSTB2022NSCQMSX1371). The authors have no other conflicts of interest to declare.

*Ethical Statement:* The authors are accountable for all aspects of the work in ensuring that questions related to the accuracy or integrity of any part of the work are appropriately investigated and resolved. All procedures performed in this study were in accordance with the ethical standards of the institutional and/or national research committee(s) and with the Helsinki Declaration (as revised in 2013). Written informed consent was obtained from the patient for the publication of this case report and the accompanying images. A copy of the written consent form is available for review by the editorial office of this journal.

*Open Access Statement:* This is an Open Access article distributed in accordance with the Creative Commons Attribution-NonCommercial-NoDerivs 4.0 International License (CC BY-NC-ND 4.0), which permits the non-commercial replication and distribution of the article with the strict proviso that no changes or edits are made and the original work is properly cited (including links to both the formal publication through the relevant DOI and the license). See: <https://creativecommons.org/licenses/by-nc-nd/4.0/>.

## References

1. Yang T, Tabrizian P, Zhang H, Lau WY, Han J, Li ZL, Wang Z, Wu MC, Florman S, Schwartz ME, Shen F. Comparison of Patterns and Outcomes of Liver Resection for Hepatocellular Carcinoma: East vs West. *Clin Gastroenterol Hepatol* 2017;15:1972-4.
2. Meng F, Zhao J, Tan AT, Hu W, Wang SY, Jin J, et al. Immunotherapy of HBV-related advanced hepatocellular carcinoma with short-term HBV-specific TCR expressed T cells: results of dose escalation, phase I trial. *Hepatol Int* 2021;15:1402-12.
3. Zhou J, Sun H, Wang Z, Cong W, Wang J, Zeng M, et al. Guidelines for the Diagnosis and Treatment of Hepatocellular Carcinoma (2019 Edition). *Liver Cancer* 2020;9:682-720.
4. Salem R, Gabr A, Riaz A, Mora R, Ali R, Abecassis M, et al. Institutional decision to adopt Y90 as primary treatment for hepatocellular carcinoma informed by a 1,000-patient 15-year experience. *Hepatology* 2018;68:1429-40.
5. Dhondt E, Lambert B, Hermie L, Huyck L, Vanlangenhove P, Geerts A, Verhelst X, Aerts M, Vanlander A, Berrevoet F, Troisi RI, Van Vlierberghe H, Defreyne L. (90)Y Radioembolization versus Drug-eluting Bead Chemoembolization for Unresectable Hepatocellular Carcinoma: Results from the TRACE Phase II Randomized Controlled Trial. *Radiology* 2022;303:699-710.
6. De la Garza-Ramos C, Montazeri SA, Croome KP, LeGout JD, Sella DM, Cleary S, Burns J, Mathur AK, Overfield CJ, Frey GT, Lewis AR, Paz-Fumagalli R, Ritchie CA, McKinney JM, Mody K, Patel T, Devic Z, Toskich BB. Radiation Segmentectomy for the Treatment of Solitary Hepatocellular Carcinoma: Outcomes Compared with Those of Surgical Resection. *J Vasc Interv Radiol* 2022;33:775-785.e2.
7. Kim E, Sher A, Abboud G, Schwartz M, Facciuto M, Tabrizian P, Knešarek K, Fischman A, Patel R, Nowakowski S, Llovet J, Taouli B, Lookstein R. Radiation segmentectomy for curative intent of unresectable very early to early stage hepatocellular carcinoma (RASER): a single-centre, single-arm study. *Lancet Gastroenterol Hepatol* 2022;7:843-50.
8. Gabr A, Polineni P, Mouli SK, Riaz A, Lewandowski RJ, Salem R. Neoadjuvant Radiation Lobectomy As an Alternative to Portal Vein Embolization in Hepatocellular Carcinoma. *Semin Nucl Med* 2019;49:197-203.
9. Gabr A, Kulik L, Mouli S, Riaz A, Ali R, Desai K, et al. Liver Transplantation Following Yttrium-90 Radioembolization: 15-Year Experience in 207-Patient Cohort. *Hepatology* 2021;73:998-1010.
10. Lewandowski RJ, Gabr A, Abouchaleh N, Ali R, Al Asadi A, Mora RA, Kulik L, Ganger D, Desai K, Thornburg B, Mouli S, Hickey R, Caicedo JC, Abecassis M, Riaz A, Salem R. Radiation Segmentectomy: Potential Curative Therapy for Early Hepatocellular Carcinoma. *Radiology* 2018;287:1050-8.
11. Kim MA, Jang H, Choi NR, Nam JY, Lee YB, Cho EJ, Lee JH, Yu SJ, Kim HC, Chung JW, Yoon JH, Kim YJ. Yttrium-90 Radioembolization Is Associated with Better Clinical Outcomes in Patients with Hepatocellular Carcinoma Compared with Conventional Chemoembolization: A Propensity Score-Matched Study. *J Hepatocell Carcinoma* 2021;8:1565-77.

12. Salem R, Johnson GE, Kim E, Riaz A, Bishay V, Boucher E, Fowers K, Lewandowski R, Padia SA. Yttrium-90 Radioembolization for the Treatment of Solitary, Unresectable HCC: The LEGACY Study. *Hepatology* 2021;74:2342-52.
13. Edeline J, Gilibert M, Garin E, Boucher E, Raoul JL. Yttrium-90 microsphere radioembolization for hepatocellular carcinoma. *Liver Cancer* 2015;4:16-25.
14. Ibrahim SM, Kulik L, Baker T, Ryu RK, Mulcahy MF, Abecassis M, Salem R, Lewandowski RJ. Treating and downstaging hepatocellular carcinoma in the caudate lobe with yttrium-90 radioembolization. *Cardiovasc Intervent Radiol* 2012;35:1094-101.
15. Liou H, Mody K, Boyle AW, Keaveny AP, Croome KP, Burns JM, Harnois DM, Patel TC, Toskich B. Neoadjuvant Radiation Lobectomy and Immunotherapy for Angioinvasive HCC Resulting in Complete Pathologic Response. *Hepatology* 2021;74:525-7.
16. Yaghamai V, Besa C, Kim E, Gatlin JL, Siddiqui NA, Taouli B. Imaging assessment of hepatocellular carcinoma response to locoregional and systemic therapy. *AJR Am J Roentgenol* 2013;201:80-96.
17. Na SJ, Oh JK, Hyun SH, Lee JW, Hong IK, Song BI, Kim TS, Eo JS, Lee SW, Yoo IR, Chung YA, Yun M. (18)F-FDG PET/CT Can Predict Survival of Advanced Hepatocellular Carcinoma Patients: A Multicenter Retrospective Cohort Study. *J Nucl Med* 2017;58:730-6.
18. Filippi L, Schillaci O, Bagni O. Recent advances in PET probes for hepatocellular carcinoma characterization. *Expert Rev Med Devices* 2019;16:341-50.
19. Kallini JR, Miller FH, Gabr A, Salem R, Lewandowski RJ. Hepatic imaging following intra-arterial embolotherapy. *Abdom Radiol (NY)* 2016;41:600-16.
20. Guo J, Seo Y, Ren S, Hong S, Lee D, Kim S, Jiang Y. Diagnostic performance of contrast-enhanced multidetector computed tomography and gadoxetic acid disodium-enhanced magnetic resonance imaging in detecting hepatocellular carcinoma: direct comparison and a meta-analysis. *Abdom Radiol (NY)* 2016;41:1960-72.
21. Suzuki C, Jacobsson H, Hatschek T, Torkzad MR, Bodén K, Eriksson-Alm Y, Berg E, Fujii H, Kubo A, Blomqvist L. Radiologic measurements of tumor response to treatment: practical approaches and limitations. *Radiographics* 2008;28:329-44.
22. Lencioni R, Llovet JM. Modified RECIST (mRECIST) assessment for hepatocellular carcinoma. *Semin Liver Dis* 2010;30:52-60.
23. Semaan S, Makkar J, Lewis S, Chatterji M, Kim E, Taouli B. Imaging of Hepatocellular Carcinoma Response After (90)Y Radioembolization. *AJR Am J Roentgenol* 2017;209:W263-76.
24. Lock M, Malayeri AA, Mian OY, Mayr NA, Herman JM, Lo SS. Computed tomography imaging assessment of postexternal beam radiation changes of the liver. *Future Oncol* 2016;12:2729-39.
25. Syed M, Shah J, Montazeri SA, Grajo JR, Geller B, Toskich B. Analysis of dynamic hepatobiliary contrast-enhanced MRI signal intensity after Yttrium-90 radioembolization with glass microspheres for the treatment of hepatocellular carcinoma. *Abdom Radiol (NY)* 2021;46:2182-7.
26. Chung J, Yu JS, Chung JJ, Kim JH, Kim KW. Haemodynamic events and localised parenchymal changes following transcatheter arterial chemoembolisation for hepatic malignancy: interpretation of imaging findings. *Br J Radiol* 2010;83:71-81.

**Cite this article as:** Li X, Yue X, Zhang L, Liu C, Wang J, Zhang H, Cai P. Imaging evaluation following transarterial radioembolization with yttrium-90 microspheres downstaging hepatocellular carcinoma: the first case in China. *Quant Imaging Med Surg* 2023;13(4):2744-2750. doi: 10.21037/qims-22-943